THE JOURNAL OF BIOLOGICAL CHEMISTRY VOL. 286, NO. 39, pp. 34457–34467, September 30, 2011

Passive Immunization with Anti-Tau Antibodies in Two Transgenic Models

REDUCTION OF TAU PATHOLOGY AND DELAY OF DISEASE PROGRESSION

Received for publication, February 10, 2011, and in revised form, August 10, 2011 Published, JBC Papers in Press, August 12, 2011, DOI 10.1074/jbc.M111.229633

Xiyun Chai[‡], Su Wu[‡], Tracey K. Murray[§], Robert Kinley[§], Claire V. Cella[§], Helen Sims[§], Nicola Buckner[§], Jenna Hanmer[§], Peter Davies[¶‖], Michael J. O'Neill[§], Michael L. Hutton[§], and Martin Citron[‡1]

From the [‡]Eli Lilly and Company, Lilly Corporate Center, Indianapolis, Indiana 46285, [§]Eli Lilly and Company, Lilly-Erl Wood Manor, Windlesham, Surrey GU20 6PH, United Kingdom, the [¶]Albert Einstein College of Medicine, Yeshiva University, Bronx, New York 10461, and the [‖]Litwin-Zucker Center for Research on Alzheimer's Disease, Feinstein Institute, Manhasset, New York 11030

Background: Recent active immunization studies have raised the possibility of modulating Tau pathology.
Results: Peripheral administration of two antibodies against pathological Tau forms reduces Tau pathology and improves functional outcomes.
Conclusion: Passive immunotherapy is effective at preventing the buildup of intracellular Tau pathology.
Significance: Tau immunotherapy should be considered as a therapeutic approach for the treatment of Alzheimer disease and other tauopathies.

The microtubule-associated protein Tau plays a critical role in the pathogenesis of Alzheimer disease and several related disorders (tauopathies). In the disease Tau aggregates and becomes hyperphosphorylated forming paired helical and straight filaments, which can further condense into higher order neurofibrillary tangles in neurons. The development of this pathology is consistently associated with progressive neuronal loss and cognitive decline. The identification of tractable therapeutic targets in this pathway has been challenging, and consequently very few clinical studies addressing Tau pathology are underway. Recent active immunization studies have raised the possibility of modulating Tau pathology by activating the immune system. Here we report for the first time on passive immunotherapy for Tau in two well established transgenic models of Tau pathogenesis. We show that peripheral administration of two antibodies against pathological Tau forms significantly reduces biochemical Tau pathology in the JNPL3 mouse model. We further demonstrate that peripheral administration of the same antibodies in the more rapidly progressive P301S tauopathy model not only reduces Tau pathology quantitated by biochemical assays and immunohistochemistry, but also significantly delays the onset of motor function decline and weight loss. This is accompanied by a reduction in neurospheroids, providing direct evidence of reduced neurodegeneration. Thus, passive immunotherapy is effective at preventing the buildup of intracellular Tau pathology, neurospheroids, and associated symptoms, although the exact mechanism remains uncertain. Tau immunotherapy should therefore be considered as a therapeutic approach for the treatment of Alzheimer disease and other tauopathies.

Over the last decade numerous clinical immunotherapy programs for Alzheimer disease (AD)[2] modification targeting amyloid-β peptide (Aβ) have emerged based on the idea that a small proportion of peripherally administered antibodies reaches the CNS and induces clearance of soluble and/or deposited extracellular Aβ by various mechanisms (1). In contrast, much less progress has been made in addressing intracellular Tau pathology, the second major hallmark of AD. Neurofibrillary inclusions containing aggregated, hyperphosphorylated Tau are defining characteristics of AD pathology and a number of other tauopathies, including Pick disease, progressive supranuclear palsy, corticobasal degeneration, and agyrophilic grain disease. In all these disorders there is a strong correlation between symptomatic progression and the level and distribution of Tau intraneuronal aggregates (2). Moreover, the discovery of mutations in the Tau gene (*MAPT*) that cause some familial forms of frontotemporal dementia provide a direct genetic link between Tau and neurological disease (3).

In its normal state, Tau is a highly soluble cytoplasmic microtubule-binding protein, which occurs in the human CNS in 6 main isoforms, ranging from 352 to 441 residues. Its main role is likely the stabilization of microtubules in axons as tracks for axonal transport and as cytoskeletal elements for growth. In AD neuronal Tau inclusions first appear in the transentorhinal cortex from where they spread to the hippocampus and neocortex. The tangles observed in AD neurons consist of hyperphosphorylated, aggregated insoluble Tau (for a recent review see Ref. 4). Direct toxic effects of the pathological Tau species and/or loss of axonal transport due to sequestration of functional Tau into hyperphosphorylated and aggregated forms, which are no longer capable of supporting axonal transport, have been proposed to contribute to disease.

To date, the identification of tractable targets to block the progression of Tau pathology has been challenging. However

[1] To whom correspondence should be addressed: Eli Lilly and Co., Lilly Corporate Center, Indianapolis, IN 46285. Tel.: 317-277-7176; E-mail: citronma@lilly.com.

[2] The abbreviations used are: AD, Alzheimer disease; Aβ, amyloid-β peptide; ANOVA, analysis of variance; Ab, antibody.

three recent active immunization studies have raised the possibility of reducing Tau pathology by activating the immune system (5–7). In this study we set out to directly explore the effect of anti-Tau antibodies on Tau pathology and associated disease using two different transgenic mouse models. Using robust biochemical assays we demonstrate for the first time a reduction in the 64-kDa hyperphosphorylated insoluble Tau species, a biochemical correlate of neurofibrillary tangles (8). Using blinded assessors and rigorous statistical analysis we show a reduction in neurofibrillary tangle pathology in the rapidly progressing P301S mouse model, which translates into a pronounced amelioration of the phenotypic progression in this model with a slowed decline in motor function and decreased weight loss.

EXPERIMENTAL PROCEDURES

Antibody Treatment Studies—We used antibodies PHF1 (which recognizes Tau with phosphorylated serines 396 and 404 (9)) and MC1 (a conformation-dependent antibody that recognizes an early pathological Tau conformation (10)) and a control mouse IgG1 from a hybridoma of mice that had not been immunized (Harlan). Antibodies were purified from ascites and were controlled for endotoxin levels (<0.19 endotoxin units/mg for both PHF1 and MC1 and for the IgG1 control antibody, <0.55 endotoxin units/mg and <0.33 endotoxin units/mg in the JNPL3 and P301S studies, respectively). In the JNPL3 study antibodies were administered at 15 mg/kg three times a week for 2 months and then at 10 mg/kg twice a week for the remaining 2 months at Covance Laboratories, Inc., Greenfield, IN. In the P301S study antibodies were administered at 15 mg/kg twice weekly. After completion of the dosing phase mice were sacrificed, and brains and spinal cords were collected.

Biochemical Assays—We developed an assay to accurately quantify the accumulation of conformationally altered hyperphosphorylated pathological Tau. Half brains and spinal cords were weighed and homogenized in 10 volumes of homogenization buffer (Tris-buffered saline (TBS), pH 7.4, containing 1× protease and phosphatase inhibitor mixture (Thermo) with 2 mM EGTA). The homogenized samples were spun at 21,000 × *g* for 20 min, the supernatants were collected (total extract), and an aliquot was saved for analysis of the starting material. The rest of the total extract was centrifuged at 100,000 × *g* for 1 h at 4 °C to obtain insoluble pellet (P1 fraction) and supernatant (S1 fraction) (Fig. 1). Our analyses in this study focused on the insoluble 64-kDa Tau species in the P1 fraction. To demonstrate that our P1 preparation is adequate, we investigated the correlation of the AT8 ELISA (see below) signal in the P1 fraction with the AT8 signal in the Sarkosyl-insoluble fraction, generated by a standard procedure (11) with slight modifications (Fig. 1). Four JNPL3 mouse brain samples with different degrees of Tau pathology were processed to generate the P1 fraction, and then these P1 samples were subjected to Sarkosyl extraction (Fig. 1). Both the P1 samples and the Sarkosyl-extracted samples were subjected to our AT8 ELISA assay, so that for each brain we obtained a P1 ELISA read (*x* axis) and then a second read after Sarkosyl ELISA extraction (*y* axis). Although the absolute AT8 signal was somewhat reduced after Sarkosyl extraction, the correlation was almost perfect, indicating that our P1 preparation was adequate (Fig. 2).

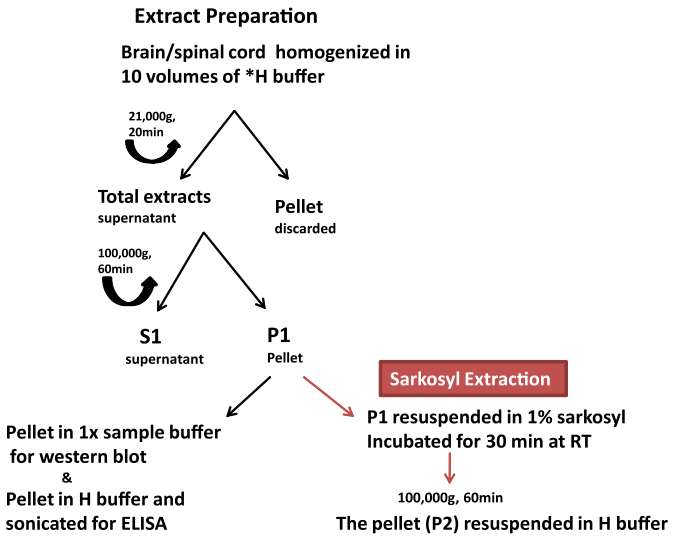

FIGURE 1. **Procedure for preparation of tissue extracts.** Most of our analyses are focused on the P1 fraction, which can be further processed by Sarkosyl extraction (11).

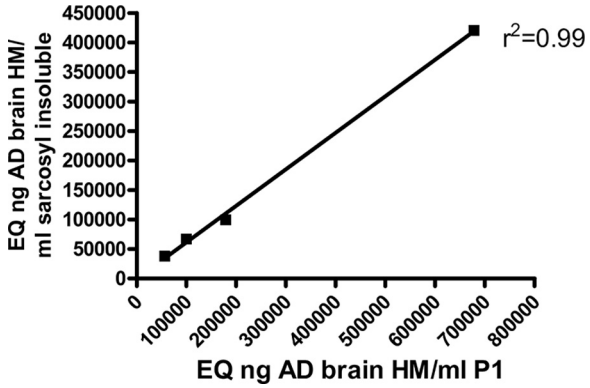

FIGURE 2. **Correlation of the AT8 signal in the P1 fraction with the AT8 signal in the Sarkosyl-insoluble fraction.** Four JNPL3 mouse brain samples with different degrees of Tau pathology were processed to generate the P1 fraction, and then these P1 samples were subjected to Sarkosyl extraction (11) (see Fig. 1). Both the P1 samples and the Sarkosyl-extracted samples were subjected to AT8 ELISA, so that for each brain there is a P1 ELISA read (*x* axis) and then a second read after Sarkosyl ELISA extraction (*y* axis). Whereas the absolute AT8 signal is somewhat reduced after Sarkosyl extraction, the correlation is almost perfect, indicating that our P1 preparation is adequate.

Western Blotting—Total extracts were analyzed for total Tau and actin using antibodies HT7 (12) and monoclonal anti-β-actin (Sigma), respectively. HT7 is a human-Tau-specific monoclonal antibody recognizing amino acids 159–163. The P1 fraction was resuspended in 1× Tris-glycine SDS sample buffer. The proteins were separated on 4–20% Tris-glycine midi gel (Invitrogen), transferred to Ibolt gel nitrocellulose using the Ibolt Dry Blotting System (Invitrogen), and probed with AT8 antibody (Thermo Scientific, 1:1000).

For quantitation we established a sandwich ELISA using AT8 for capture and the pan-Tau antibody CP27 (13) for detection. AD brain homogenates were used for standard curves. To quantify the AT8 signal in the P1 fraction, the P1 pellet prepared above was washed three times with 0.5 ml of 1× cell lysis buffer (Cell Signaling) supplemented with protease inhibitor mixture (Roche Applied Science). The pellet was resuspended in 0.5 ml of cell lysis buffer by sonication.

AT8 ELISA Assay—A 96-well half area high binding ELISA plate (Costar) was coated with 2 μg/ml AT8 antibody (13) in PBS overnight at 4 °C. The plate was washed with PBS buffer containing 0.05% Tween 20 (PBST) three times and blocked with BB3 blocking buffer (ImmunoChemistry Technology). For standard curves, an AD brain homogenate (800 $\times$ *g* supernatant) at 40 μg/ml was 2-fold serially diluted with 0.25% casein buffer. We then plotted all brain extract ELISA assays as nanogram or microgram AD brain homogenate that would produce the same ELISA signal. The plates with standard and samples were incubated at 4 °C overnight and washed with PBST for four times. As primary antibody CP27-biotin (13) at 1:4000 dilution in 0.25% casein buffer was added to the plate and incubated at room temperature for 2 h, followed by four PBST washes. Streptavidin-HRP (BioSource) in a 1:10,000 dilution in 0.25% casein buffer was added and incubated at room temperature for 1 h. The plate was washed four times with PBST, and a 1:1 mixture of 3,3′,5,5′-tetramethyl benzidine and H_2O_2 (Thermo Scientific) was added to the plate, and the mixture was incubated at room temperature for 10 min. The reaction was stopped by adding 2 N H_2SO_4.

AT8 ELISA Spike Assay and Specificity Assay—To test if PHF1 and MC1 antibodies (which both recognize Tau epitopes different from AT8 and CP27) interfere with the AT8 ELISA assay, a spike experiment was carried out by adding PHF1 or MC1 antibody in a JNPL3 brain P1 sample at a final concentration of 1.25, 2.5, or 5 ng/ml. Based on previous experience that a 40 mg/kg IgG injection in mice leads to peak plasma levels of ~250 μg/ml, we calculated that spiking 5 ng/ml exceeds the highest possible antibody level in the P1 sample used for ELISA by almost 10-fold. Assuming that cerebrospinal fluid IgG concentration is ~0.1% of plasma concentration and that cerebrospinal fluid concentration roughly equals brain concentration, one would expect ~250 ng/ml in brain. Assuming that all of the brain antibody is captured in the P1 pellet and factoring in all dilution steps, the maximal antibody concentration in the ELISA mixture would be 0.6 ng/ml. The calculated AT8 signals in the spiked samples were normalized to the control JNPL3 brain P1 sample and expressed as a percentage of control. For the specificity assay a normal human brain homogenate and an AD brain homogenate (used as standard for the AT8 ELISA assay) were diluted to 40 μg/ml in 0.25% casein buffer, and 2-fold serial dilutions in the same buffer were made. The AT8 assay was carried out as described above. The A_{450} was plotted against the protein concentration of the brain homogenates. Tau_{441} recombinant standard (rPeptide) was tested at various concentrations and did not produce an AT8 signal in our ELISA (not shown).

Immunohistochemistry—Brains were hemi-dissected and placed in 10% buffered formalin. After processing (Tissue TEK®) and embedding, 8-μm sagittal sections were cut using a rotary microtome (Microm, HM200). These sections were subsequently stained using the following primary antibodies: AT8 (1:4000, Innogenetics), PG5 (1:500, Peter Davies), nY29 (1:5000, Covance), NF200 (for 200-kDa neurofilament, 1:1000, Millipore). To examine the effects of treatment on astrocyte and microglia responses we used primary antibodies to glial fibrillary acidic protein (1:1, Biogenix, ready to use) and to ionized calcium-binding adaptor molecule 1 (1:5000, Wako). Secondary antibody was applied, and slides were then incubated with avidin-biotin complex reagent for 5 min. After rinsing, slides were treated with the chromogen 3,3′-diaminobenzidine (Vector Laboratories, SK-4100) to allow visualization. The slides were then covered with coverslips, dried, and digitized using an Aperio Scanscope XT (Aperio Technologies). The number of Tau-positive cells was quantified in the brain stem using ImagePro Plus software. This work was carried out by investigators who were blinded to the treatment status of the mice.

Rota-Rod Assay—Rota-Rod performance was used to assess balance and hind limb motor function using an ENV-575MA five-station mouse Rota-Rod (Med Associates Inc.). Mice were placed on a rotating rod, and the time each mouse was able to maintain its balance walking on top of the rod was recorded. Mice were initially trained for 4 trials per day for 3 consecutive days at a fixed speed of 20 rpm. Some mice hold on to the rotating rod as they begin to lose their balance and ride completely around the rod rotating with it. For these mice, the latency to the first complete revolution was recorded and they were removed from the Rota-Rod. On completion of training mice were assessed at five different speeds (16, 20, 24, 28, and 32 rpm) on 2 separate trials for a maximum trial length of 60 s, and the latency to fall was recorded. Rota-Rod performance was assessed prior to initiation of antibody treatment when the mice were 2 months old and then at 3.5, 4, 4.5, and 5 months old.

Statistical Analysis: Brain ELISA Assays—We used Dunnett's test to adapt analysis of variance for our scenario, comparing each treatment group with a control group. One requirement for analysis of variance to be valid is that the data are (at least approximately) normally distributed. In a biological setting it is often the case that treatment effects are proportional, rather than additive, in which case it may be found that, although the raw data are not normally distributed, their logarithms are. This is the case with the present ELISA data sets, as was verified by carrying out goodness-of-fit tests for both the raw results and their logarithms (base 10) in each of the treatment and control groups. For the logged results the hypothesis of Normality is not rejected for any group, while for the raw results Normality is rejected in some groups. The statistics for the ELISA assays shown in Figs. 6 and 9 are therefore done with the logged results.

Data are presented as mean $\pm$ S.E. and p values of <0.05 being considered statistically significant. Immunohistochemistry data were analyzed (Statistica, StatSoft Inc.) using analysis of variance (ANOVA), and where appropriate, followed by post-hoc Dunnett's test. Changes in body weight were evaluated using a repeated-measures ANOVA performed on transformed data [square root (change in body weight compared with day 1 + 10)] with GROUP as the between-subjects factor and TIME as the repeated measure. If a significant GROUP $\times$ TIME interaction was observed, univariate planned comparisons was used to determine at which time point groups differed followed by post-hoc Dunnett's test. Rota-Rod data were initially transformed (square root) followed by repeated-measures ANOVA and post-hoc Dunnett's test.

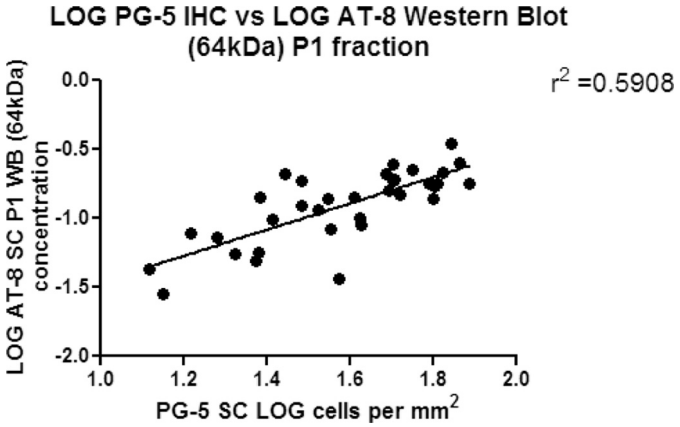

FIGURE 3. **Correlation of the 64-kDa P1 Tau species on Western blots with neurofibrillary tangles (as detected by immunohistochemistry with antibody PG5).**

RESULTS

We administered antibodies against pathological forms of Tau protein by intraperitoneal injection in mice transgenic for human mutant Tau. In the first study we used the well characterized JNPL3 mice, which express 0N4R human Tau with the P301L mutation that causes frontotemporal dementia in humans under control of the mouse prion promoter at average levels similar to endogenous mouse Tau. These mice show an age-dependent development of neurofibrillary tangles and in later stages motor neuron loss that is associated with the onset of progressive motor dysfunction (14). Biochemically, the major accumulating hyperphosphorylated Tau species migrates with an apparent molecular mass of 64 kDa and is found almost exclusively in insoluble fractions. Significantly this species in JNPL3 mice comigrates with hyperphosphorylated, insoluble forms of 4R0N Tau from human AD brain (so-called "PHF" Tau) on SDS-PAGE. This Tau species accumulates in AD (and in all other human tauopathies), and as with the mice this is absent in normal individuals. Moreover the 64-kDa species displays the typical phosphoepitope profile of human PHF Tau (15) and correlates with functional deficits in several models of tauopathy (16). This band is thus the biochemical correlate or remnant of neurofibrillary tangles and earlier pathological Tau assemblies that are sensitive to SDS and that are therefore broken down during the process of Western blot analysis (8).

Levels of this species correlate closely with neurofibrillary tangle counts in transgenic models as the mice age and their phenotype develops. We show this here for P301S mice (Fig. 3). Moreover propagation of Tau pathology by injecting normal mice with brain extracts from P301S mice can only be achieved if extracts containing the 64-kDa Tau species are used (8). As a result the relevance of measuring the levels of this species in our transgenic mice, especially to assess the impact of immunotherapy, is clear.

In a pilot study, using JNPL3 mice, we established a treatment window by demonstrating that in our colony male homozygous mice do not show insoluble 64-kDa Tau in brain at 2 months of age but that it can be detected at 5 months of age (not shown). We then initiated the first study, in which JNPL3 mice were treated from 2 to 6 months of age with either one of two different mouse monoclonal antibodies that detect epitopes enriched in pathological Tau: PHF1 (which recognizes Tau with phosphorylated serines 396 and 404 (9)) or MC1 (a conformation-dependent antibody that recognizes an early pathological Tau conformation (10)) or a control mouse IgG1 antibody.

At the end of the study half brains were homogenized to generate a total extract, and we then separated the soluble fraction (S1) from the insoluble fraction (P1). For the JNPL3 mouse we focused our analysis of Tau immunotherapy effects on the P1 fraction, because in this model the 64-kDa pathological Tau species is found almost exclusively in this fraction. Western blot analysis of this fraction using antibody AT8 (which recognizes Tau phosphorylated at Ser-202 and Thr-205 (17)) showed only the 64-kDa Tau band, which exhibited substantial animal-to-animal variability, but overall was reduced in both the PHF1- and MC1-treated groups *versus* control (Fig. 4*A*). In contrast, in the total brain extract, total human Tau, as detected by Western blotting with antibody HT7 (a human-specific monoclonal antibody recognizing amino acids 159–163 (12)), appeared similar in all groups (Fig. 4*B*), indicating that the observed reduction of the 64-kDa band was not simply a consequence of reducing overall Tau levels.

To rigorously quantitate pathological Tau burden in our models, we established an ELISA assay method using AT8 as capture antibody (see "Experimental Procedures"). This assay showed a broad dynamic range and did not detect normal brain Tau (Fig. 5*A*) or recombinant wild-type Tau (not shown). Such an assay should allow more accurate quantitation than scanning of Western blots with a quite limited dynamic range. Moreover, linking the AT8 ELISA to our relatively simple fractionation procedure enables a robust biochemical assessment of the Tau pathology in our transgenic models. As expected, comparing the AT8 ELISA readouts *versus* quantitation of the 64-kDa band in AT8 Western blots of the P1 fraction of all animals in the study showed a strong correlation (Fig. 5*B*, $r^2 = 0.73$).

Spiking experiments further demonstrated that neither MC1 nor PHF1 interfered with this assay (Fig. 5*C*). This is an important control, because the brains and spinal cords of the treated mice may contain treatment antibodies that could be released during the extraction. Using this AT8 ELISA for the insoluble fraction of the brain we found that both antibodies reduced the biochemical pathology by >50% (Fig. 6*A*), which was highly statistically significant ($p = 0.0006$ for PHF1 and $p = 0.0004$ for MC1 by Dunnett's method (Fig. 6*B*)). Applying the same analysis techniques to spinal cords of the same mice we obtained similar results with significant reductions for both PHF1 and MC1 treatment *versus* control antibody (not shown).

This is the first demonstration that Tau immunotherapy is able to reduce the accumulation of biochemically measurable pathological Tau species. However, these data also point to the high inter-animal variability in the Tau pathology observed in the JNPL3 model, which has been reported before (18) and which makes interpreting pharmacological studies extremely difficult. Moreover, JNPL3 mice on the available genetic background display very slow pathogenic progression with only

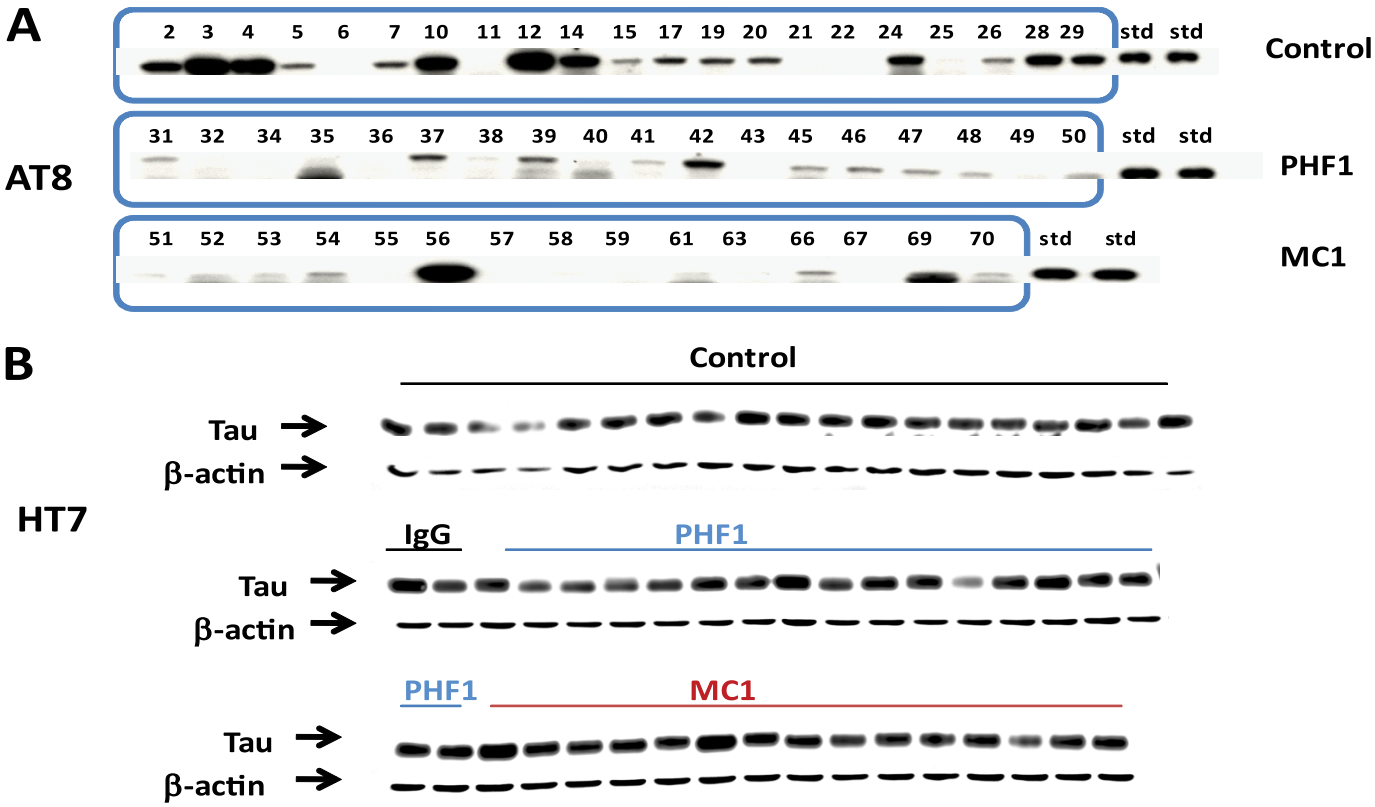

FIGURE 4. **Biochemically detectable Tau pathology in JNPL3 mice is reduced after passive immunization with anti-Tau antibodies.** *A*, AT8 Western blot of the P1 brain fraction from 6-month-old JNPL3 mice shows the specificity of the antibody for the 64-kDa band of hyperphosphorylated human Tau that comigrates with PHF Tau from AD brain (15) and correlates with functional deficits in several models of tauopathy (16). The 64-kDa band is weaker in the MC1 and PHF1 treatment groups compared with control antibody. *B*, HT7 Western blot of total Tau in total extracts shows no apparent differences between treatment groups.

sparse tangles detectable by immunohistochemistry until the mice are more than a year old. As a result this model is also not ideally suited for investigating treatment effects on functional outcomes, as motor function is again impaired only in old mice (>1 year old) (14).

We therefore sought to confirm and extend the findings in a second model, the more recently described P301S transgenic mouse line that expresses under control of the murine thy1 promoter the 4R0N isoform of human Tau with the P301S mutation. At 5–6 months of age, homozygous animals from this line develop a neurological phenotype dominated by severe paraparesis caused by neurodegeneration in the spinal cord. As in the JNPL3 mice Sarkosyl-insoluble Tau from brains and spinal cords of the P301S mice runs as a hyperphosphorylated 64-kDa band comigrating with human PHF Tau (19). P301S mice were therefore treated from 2 to 5 months of age with either one of the two different mouse monoclonal antibodies used in the previous JNPL3 study (PHF1 or MC1) or the control mouse IgG1 antibody.

Baseline motor function was assessed prior to the start of chronic dosing, and behavior was monitored during the course of the study. The study was terminated when a major proportion of the mice began to show motor symptoms at 5 months of age. During the course of the study, the young mice in all treatment groups initially gained weight. In contrast, as motor functions became progressively impaired (4.5–5 months) all groups began to lose weight. However, there was a significant attenuation of weight loss in both the PHF1 and the MC1 treatment groups relative to control (Fig. 7*A*) with significantly delayed onset of body weight loss in both treatment groups (Fig. 7*B*).

When the motor function of the mice was assessed by Rota-Rod 1 week before sacrifice by assessors blinded to the treatment status of the mice, both the PHF1- and the MC1-treated mice outperformed the control antibody-treated mice, as shown by increased fall latency at all speeds tested (Fig. 8). After sacrifice one half brain was used for biochemistry analysis, while the other half was kept for immunohistochemistry. As in the JNPL3 study total human Tau in the total extract, as detected by Western blotting with antibody HT7, appeared similar in all groups (Fig. 9*A*), indicating that PHF1 or MC1 treatment had not substantially reduced overall Tau levels.

In contrast to the JNPL3 model the P301S mice accumulate detectable levels of hyperphosphorylated Tau species (64 kDa) in soluble as well as insoluble fractions (see "Experimental Procedures"), although as in the JNPL3 model much higher levels were again found in the insoluble fraction (~90%) and the appearance of the 64-kDa band in the soluble fraction in P301S mice was tightly correlated with levels of this species in the P1-insoluble fraction (not shown).

The precise reason for this difference between the pathological Tau accumulation in the two models is unclear, however, the rate of pathogenesis and phenotypic progression in the P301S mice is higher than in the JNPL3 mice, which may explain the apparent discrepancy (19). Therefore, we analyzed

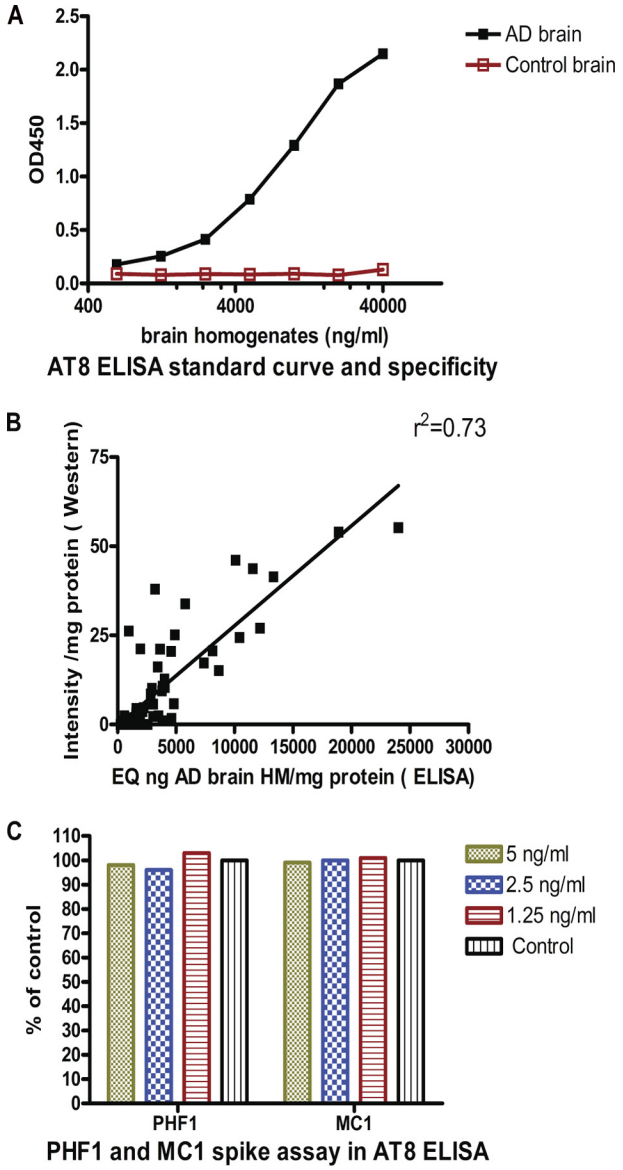

FIGURE 5. **AT8 ELISA.** *A*, standard curve using AD and control brain homogenates. The normal Tau present in control brain does not lead to a detectable signal. *B*, AT8 Western blot and ELISA results in the P1 fraction of all mice in the study show a strong correlation (r^2 = 0.73) between the two measures. *C*, spiking experiment. Addition of PHF1 and MC1 at the indicated concentrations to JNPL3 P1 extracts does not interfere with signal detection by the AT8 ELISA, demonstrating that AT8 signal changes in brains of mice treated with these antibodies are not ELISA artifacts.

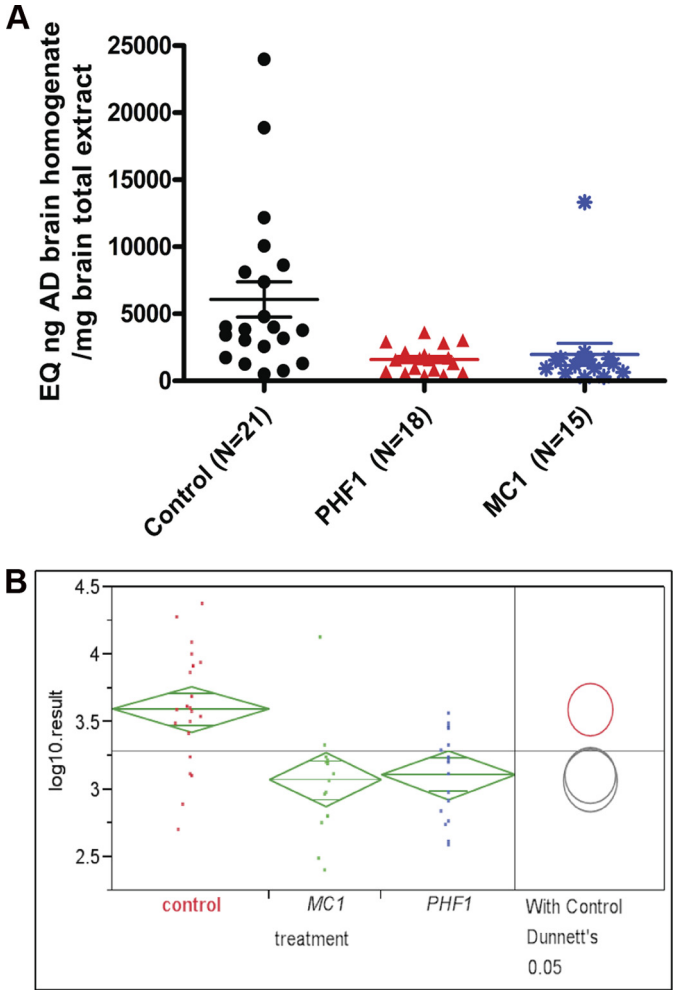

FIGURE 6. *A*, AT8 ELISA analysis of the JNPL3 mouse P1 brain fraction shows strong reduction in AT8 signal in both antibody treatment groups compared with control antibody. *B*, statistical analysis of the log-transformed AT8 ELISA data shows that the reduction is highly significant for both PHF1 and MC1.

the effects of immunotherapy on both S1 and P1 fractions. ELISA analysis of the P1 fraction (Fig. 9*B*) revealed relative to control antibody a 45% reduction in biochemical pathology in the PHF1-treated mice, which was highly significant (p = 0.006) and a 33% reduction in the MC1 group, although this was not significant at the p = 0.05 level (p = 0.088). ELISA analysis of the S1 fraction demonstrated relative to control antibody a 40% reduction with PHF1, which was significant (p = 0.037) and a 29% trend to reduction with MC1 (p = 0.138) (Fig. 9*C*).

Applying the same analysis techniques to the spinal cord P1 fraction of the same mice we obtained similar results with reductions for both PHF1 (p = 0.086) and MC1 (p = 0.016) treatment *versus* control antibody (Fig. 9*D*). In summary, in the P301S model in all fractions, where it can be detected, biochemical Tau pathology was reduced by Tau immunotherapy, consistent with the results in the JNPL3 model (see above). The P301S model showed more severe Tau histopathology at an earlier age than the JNPL3 model, and by 5–6 months many nerve cells in brain and spinal cord are strongly immunoreactive for hyperphosphorylated Tau. Moreover, the appearance of this histopathology is tightly correlated with the appearance of the 64-kDa hyperphosphorylated Tau, which can be detected biochemically (Ref. 19 and data not shown). We therefore sought to determine the effects of Tau immunotherapy not only with sensitive biochemistry methods, but also using immunohistochemistry focusing on brain stem and spinal cord, the regions that show the most robust Tau pathology in this model (19). This analysis, carried out by investigators that were blinded to the treatment status of the mice, showed evidence of reduced Tau neurofibrillary pathology in both the PHF1 and MC1 treatment groups relative to the control group using antibody PG5, which recognizes Tau phosphorylated at Ser-409 (10) (Fig. 10).

Quantitative analysis demonstrated reduction in pathology using three different detection antibodies: AT8, which recog-

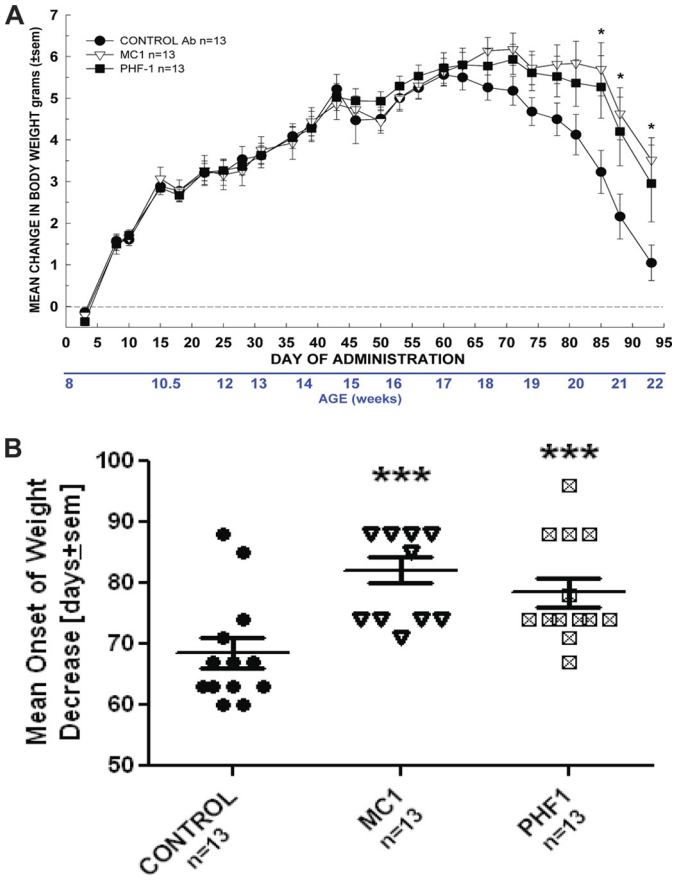

FIGURE 7. **Attenuation of body weight loss (*A*) and delay in onset of weight loss (*B*) after treatment with MC1 and PHF1.** *A*, repeated-measures ANOVA indicated that there was a significant Day × Group interaction $F(50,900) = 3.29$, $p < 0.0001$ with both MC1 and PHF1 treatment reducing the weight loss from day 85 onward. Univariate planned comparisons revealed significant group effect from day 85 onward, $p < 0.03$. Post hoc Dunnett test compared with control antibody (Ab)-treated group: Day 85: $F(2,36) = 4.07$, $p = 0.03$, MC1 $p = 0.01$, PHF1 $p = 0.03$; Day 88: $F(2,36) = 3.75$, $p = 0.03$, MC1 $p = 0.01$, PHF1 $p = 0.04$; Day 93: $F(2,36) = 4.00$, $p = 0.03$, MC1 $p = 0.009$, PHF1 $p = 0.05$. In all cases; *, $p < 0.05$ *versus* control Ab-treated. Data are based on $n = 13$ mice per group. *B*, illustrates the mean day of onset of body weight loss in P301S mice. Results indicated that both MC1 and PHF1 treatment delayed the onset of weight loss. One-way ANOVA $F(2,36) = 9.33$, $p < 0.001$. Post hoc Dunnett test compared with control Ab-treated group; ***, $p < 0.005$. Data are based on 13 mice per group.

nizes Tau phosphorylated at Ser-202 and Thr-205 (Fig. 11*A*, significant reduction for both antibodies in both regions); PG5 (10) (Fig. 11*B*, significant reduction for both antibodies in both regions), and nY29, which detects Tau nitrated at position 29 (20) (Fig. 11*C*, strong trend for both antibodies in both regions). The PG5 and nY29 antibodies each recognize epitopes that are largely restricted to neurofibrillary inclusions (tangles and neuropil threads) (10, 20).[3]

We then counted neurons in brain stem and spinal cord, but did not see a significant difference between treated and control groups, thus excluding the possibility that the observed decrease in the number of phosphorylated Tau-positive neurons could result from accelerated neuronal loss at the time points we studied.

We also addressed, immunohistochemically, whether the observed phenotypic improvements correlated with a reduction in neurospheroids in spinal cord axons as a measure of early neurodegenerative change (Fig. 12). This analysis demonstrated a significant reduction in neurospheroid numbers in mice treated with PHF1 ($p = 0.012$) and MC1 ($p = 0.004$). Finally, after staining with ionized calcium-binding adaptor molecule 1 for microglia and glial fibrillary acidic protein for astrocytes we did not find evidence of a persistent increase in astrocyte or microglia activation in treatment *versus* control groups (data not shown).

DISCUSSION

In summary, we have established that passive immunization with antibodies that selectively recognize pathological forms of Tau reduces the extent of biochemically detectable Tau pathology in two different mouse models and that this translates into a reduction in axonal degeneration, a preservation of motor function, and slowing of disease progression in the P301S model of tauopathy. The therapeutic effects observed in the P301S mice are all the more impressive given the aggressive disease course in this model. We observed strong effects on Tau pathology using both immunohistochemistry with antibodies that selectively recognize neurofibrillary inclusions and through analysis of a biochemical correlate of Tau pathology (64-kDa hyperphosphorylated tau). This assessment of two tightly linked pathological endpoints provides the most robust evidence to date that immunotherapy can slow the progression of Tau pathogenesis. Because we did not dissect brain subregions for biochemistry, we do not know whether the observed reduction in insoluble hyperphosphorylated Tau occurred to the same extent everywhere (whereas total Tau was unchanged in every brain subregion); however, immunohistochemistry in the cortex/forebrain did show a trend toward reduction of tangles in this subregion (data not shown). We chose not to cover these results in depth, because tangle numbers were variable in the cortex/forebrain of P301S mice, and those in the hippocampus were present in extremely low numbers, making interpretation of the findings in these brain regions difficult. However, overall, our data point to a broad therapeutic effect of immunotherapy with a reduction in Tau pathology observed in many of the brain regions previously reported to be impacted in the P301S model (19).

In the P301S mice, we also observed reduced numbers of neurospheroids in the spinal cords of treated mice, consistent with a therapeutic effect of Tau immunotherapy on the neurodegenerative process in this model. This in turn was linked to a clear slowing of phenotypic progression with delayed development of motor deficits and body weight loss in P301S mice treated with both Tau monoclonal antibodies. In combination, these findings indicate that the observed reduction in Tau pathology in P301S mice treated with the two Tau therapeutic antibodies also led to improved neuronal function. We did not however observe significant differences in the numbers of dorsal horn motor neurons in spinal cords from treated *versus* untreated mice despite previous reports that this model develops significant neuronal loss in this region (19). One obvious explanation, given the observed reduction in neurospheroids, is that the mice were sacrificed at a relatively early phenotypic stage prior to the onset of massive neuronal cell body loss

[3] P. Davies, unpublished data.

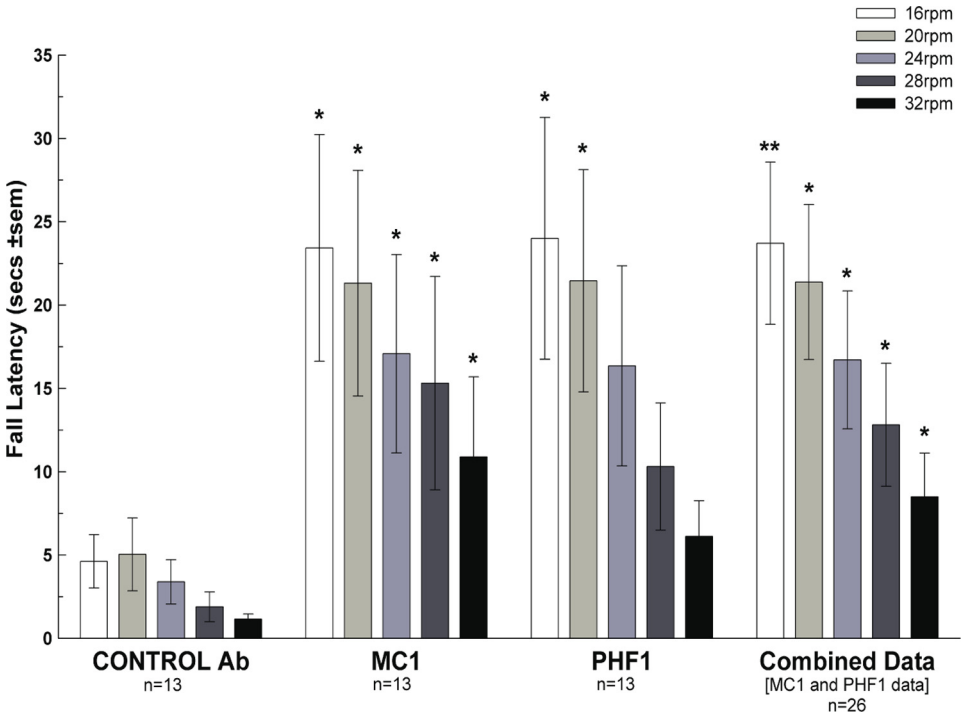

FIGURE 8. **Motor performance as measured by fall latency on Rota-Rod 1 week before sacrifice is improved by both PHF1 and MC1 *versus* control antibody treatment.** Univariate planned comparisons revealed significant difference between control Ab-treated ($n = 13$) and Combined data ($n = 26$) compared with control Ab-treated group; *, $p < 0.05$; **, $p < 0.01$. For individual PHF1 and MC1 data there were significant improvements over control Ab-treated at several speeds using post hoc Dunnett's *t* test; *, $p < 0.05$; **, $p < 0.01$.

thereby preventing the observation of a therapeutic effect on motor neuron numbers. Additional studies in this and other transgenic models will be needed to fully determine the extent to which passive immunotherapy is able to block Tau-associated neuronal loss.

It is interesting to note that both therapeutic Tau antibodies, despite recognizing very different pathological epitopes, produced very similar levels of phenotypic improvement. However, whether this reflects a maximal therapeutic effect with immunotherapy in this model awaits the outcome of studies with additional antibodies. Currently we do not understand the role of the antibody epitope for *in vivo* efficacy: Will it be necessary to target a conformational (MC1) or phospho- (PHF1) epitope found selectively in pathological forms of Tau or will a broad spectrum of antibodies show activity? *In vivo* studies with a range of different antibodies will be required to address such questions.

Four previously published active immunization studies (5–7, 21) have pointed to the possibility that Tau immunotherapy could affect Tau pathology, but the interpretation of these data has been challenging. In the first publication immunization of wild-type mice with full-length Tau emulsified with complete Freund's adjuvant, and pertussis toxin caused encephalomyelitis accompanied by the formation of neurofibrillary tangles-like pathology (21), whereas a second study from the same group, immunizing Tau transgenic mice with a mixture of three shorter phospho-Tau peptides and the same adjuvants, found no adverse symptoms, but actually showed reduction of neurofibrillary tangle pathology and increased microglial activation by immunohistochemistry (6). A second group immunized young JNPL3 mice with a phospho-Tau peptide and Adju-Phos adjuvant and observed improvement in tangle-related motor behaviors and some reduction of Tau pathology, as assessed by immunohistochemistry, whereas Western blot analysis of Tau pathology was less conclusive (5). Using the same immunogen in a new mouse model transgenic for both Tau and mutant presenilin1 (but not amyloid precursor protein), this group recently reported prevention of cognitive decline and significantly reduced PHF1 staining by immunohistochemistry in the immunized mice but no significant reduction of insoluble Tau by Western blot analysis with PHF1 antibody. Interestingly, and in contrast to Ref. 6, no significant difference was observed between immunized and control mice in the degree of microgliosis (7).

These results suggest the potential of Tau immunotherapy, but underscore the challenges of interpreting active immunization studies, where multiple components of the immune system are activated, vastly different outcomes are observed with different immunogens (full-length Tau (21) *versus* phosphopeptides (5–7)), titer responses vary between individuals, adjuvant effects may play a role, and autoantibodies complicated the characterization of the antibodies that were generated toward the immunogen (5).

With a passive immunization approach we were able to unambiguously ascribe the observed effects to two well characterized monoclonal antibodies, PHF1 and MC1. Given the combination of pathological and functional outcome measures used in our study, we are confident that the observed effects of Tau immunotherapy are robust. However, the exact mechanism by which Tau antibodies impact the development of intracellular Tau pathology is not fully understood. We also do not know whether endogenous normally functioning Tau proteins

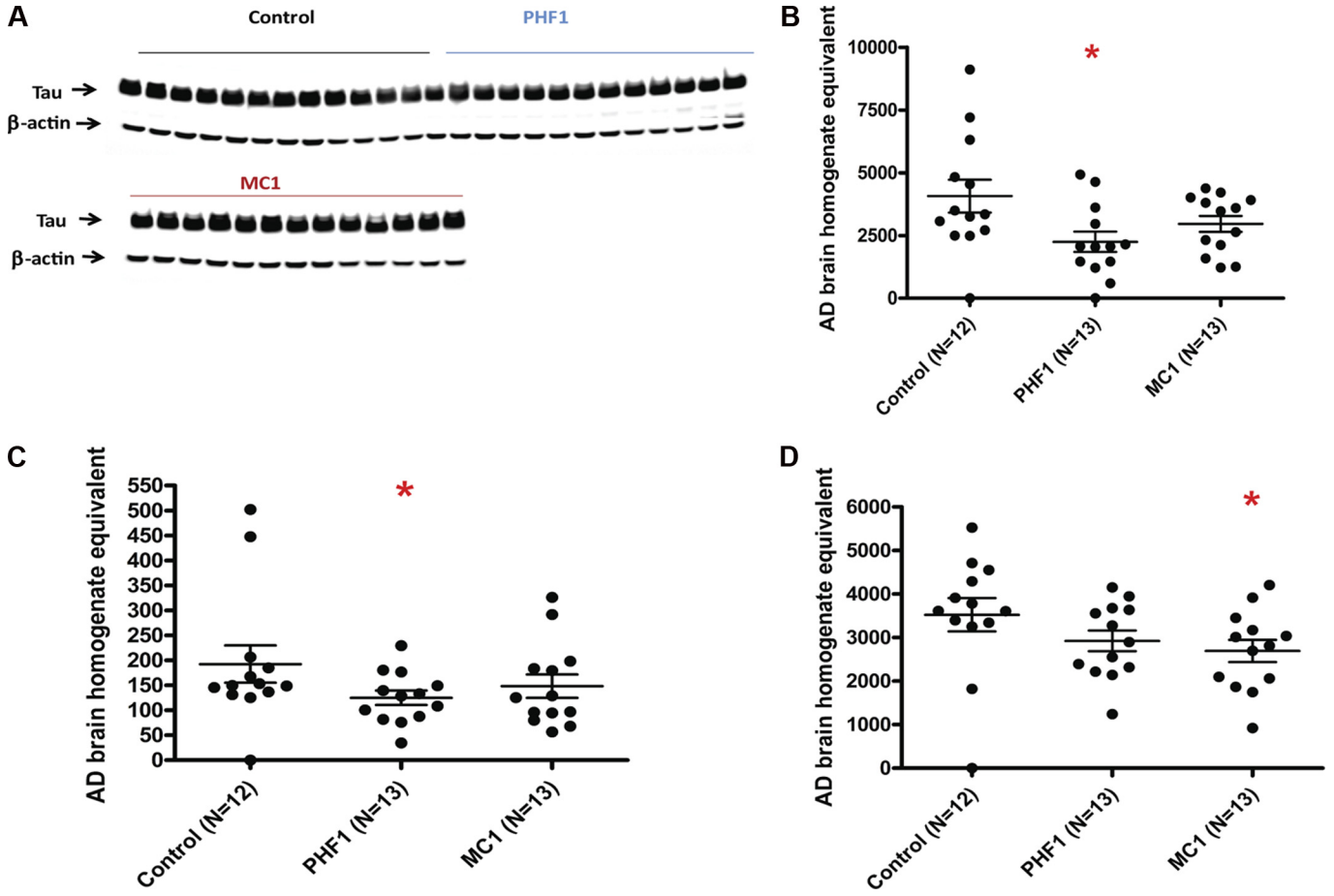

FIGURE 9. **Biochemical analysis of P301S extracts.** *A*, HT7 Western blot of total Tau in total extracts shows no apparent differences between treatment groups. *B–D*, AT8 ELISA of P301S mice. All plots show AT8 signal (micrograms of AD brain homogenate that would produce the same ELISA signal) per milligram of mouse tissue homogenate. *B*, P1 brain fraction shows a significant reduction in AT8 signal for PHF1 and a trend toward reduction for MC1 compared with control antibody. *C*, S1 brain fraction shows a significant reduction in AT8 signal for PHF1 and a trend toward reduction for MC1 compared with control antibody. Note that the AT8 signal in the soluble fraction is <10% of the P1 signal. *D*, P1 spinal cord fraction shows a significant reduction in AT8 signal for MC1 and a trend toward reduction for PHF1 compared with control antibody.

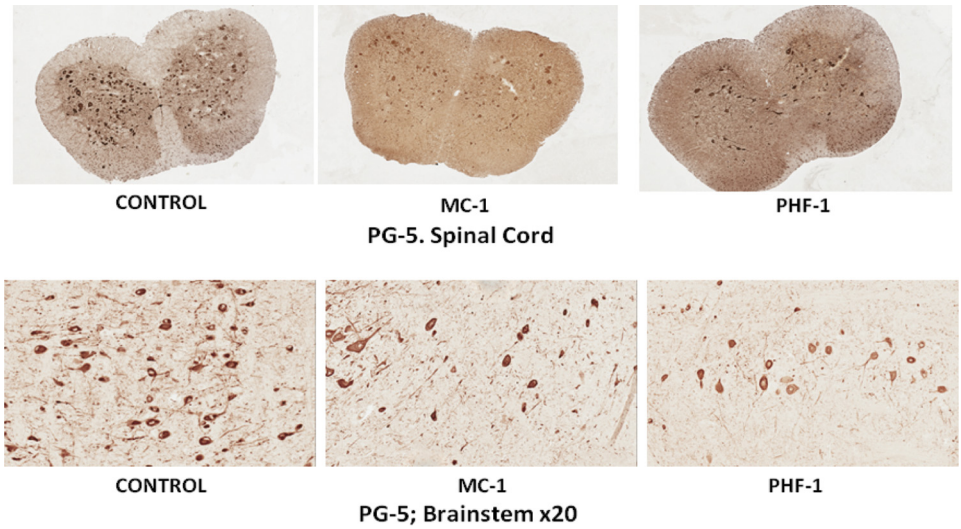

FIGURE 10. **Representative images taken from the spinal cord and brain stem (×20) from P301S mice treated with control, MC1, and PHF1 antibodies.** The *images* show a reduction in PG5 staining in the MC1- and PHF1-treated mice compared with control antibody-treated mice.

were affected by the antibody treatments. We believe that this is unlikely given that the antibodies used in our study are selective for pathological Tau and that our antibodies may not reach Tau inside the neurons, where endogenous Tau is supposed to exert its physiological function. Moreover we did not observe any negative effects on motor function in young treated P301S mice

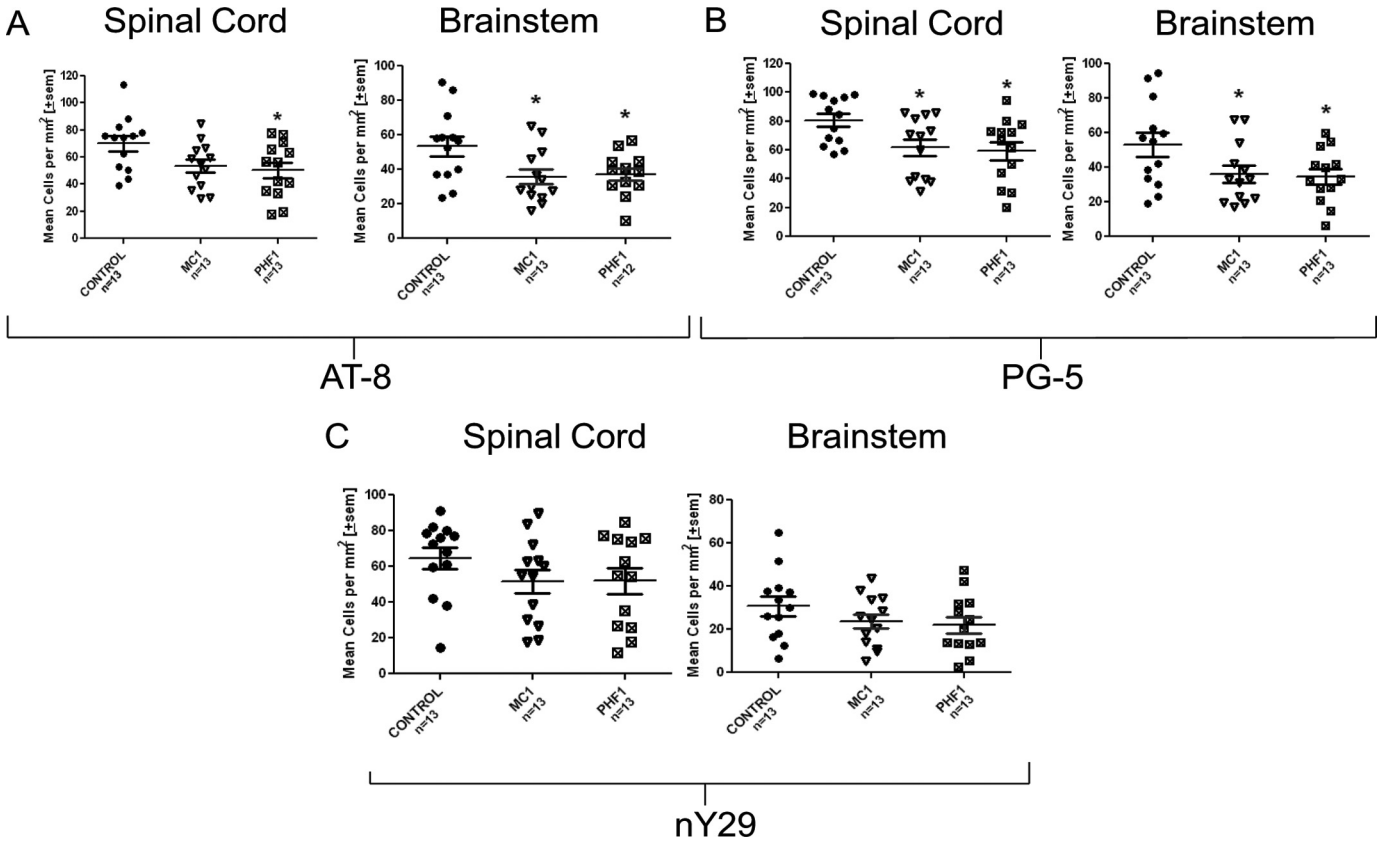

FIGURE 11. **Quantitative analysis of pathology in the spinal cord and brain stem of P301S mice.** *A*, quantitation of AT8-positive cells in brain stem shows a significant reduction for PHF1 and MC1 treatment compared with control antibody. There was also a significant reduction in of AT8 in the cord for PHF1-treated mice. *B*, quantitation of PG5 positive cells in brain stem and spinal cord shows a significant reduction for PHF1 and MC1 treatment compared with control antibody. *C*, quantitation of nY29-positive cells in spinal cord brain stem shows a trend toward reduction for PHF1 and MC1 treatment compared with control antibody. Data were analyzed using one-way ANOVA followed by post-hoc Dunnett test; *, $p < 0.05$ *versus* control antibody.

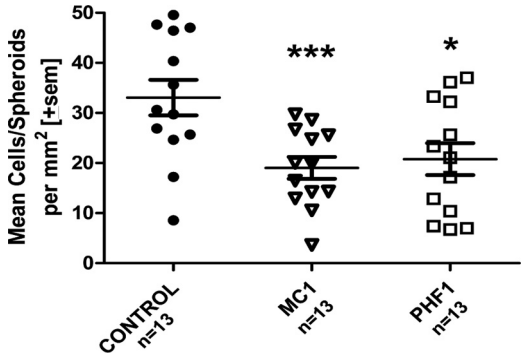

FIGURE 12. **Quantitative analysis of the number of neurofilament-positive axonal spheroids in the spinal cord of P301S mice.** Data indicated that there was a significant reduction in NF200-positive neurospheroids in the spinal cord for PHF1 and MC1 treatment compared with control. Data were analyzed using one-way ANOVA followed by post-hoc Dunnett test. *, $p < 0.05$ *versus* control antibody.

prior to the onset of the phenotype in the control animals (not shown). In addition, there was no detectable reduction in total Tau associated with immunotherapy in either model (Figs. 4 and 9).

Our study demonstrates that certain Tau antibodies alone are sufficient to drive the therapeutic effect and that other elements of the immune response to an active immunization (*e.g.* T-cell activation) are not required. We also did not find evidence of increased microglia or astrocyte activation, which appears to be critical for the mechanism of action of at least some anti-Aβ antibodies (22, 23), in the treatment *versus* control groups; however, we cannot rule out transient microglia activation that may no longer be detectable at the end of the study.

In the simplest mechanistic scenario peripherally administered anti-Tau antibodies would capture extracellular pathogenic Tau molecules and thus delay the spread of tauopathy by propagation. This scenario is supported by the following findings: First, it has long been established that a small proportion of a peripherally administered antibody dose does enter the central nervous system (22). This is independent of the epitope and just a function of the size of the protein. For example cerebrospinal fluid levels of IgGs are ~0.1% of their plasma levels (24). Second, Tau pathology can be transferred between cells in culture (25). Third, an obligatory extracellular intermediate may be necessary for the spread of tauopathy *in vivo* (26). Indeed, insoluble Tau extracts from P301S transgenic mice containing the 64-kDa hyperphosphorylated Tau species, which was reduced by passive immunotherapy in this study, were necessary and sufficient to drive the propagation of neurofibrillary pathology in the brains of recipient mice (26).

The proposed most parsimonious scenario would therefore require antibodies to get access to extracellular pathological Tau species in the CNS that underlie the spread of Tau pathology, but it would not require antibodies to directly bind intra-

neuronal Tau. It is even conceivable that exogenous antibodies transferred to cerebrospinal fluid may capture soluble, but pathological Tau species, reducing the spread of pathology by acting as a sink. This would be reminiscent of the proposed mechanisms of antibody-mediated reduction of extracellular Aβ amyloid. However, our data do not rule out more complicated mechanisms where antibodies somehow get access to intracellular Tau to block its aggregation or trigger its clearance.

Although better understanding of the mechanism of action will be important for the generation of antibodies with the best combination of epitope, affinity, and effector functions, the present data already suggest that anti-Tau antibodies may have utility for the treatment of AD, where non-amyloid-directed therapeutics are urgently needed, and also for the treatment of the less common tauopathies, where few tractable targets currently exist.

Acknowledgments—We thank Mark Ward for assistance with processing and sectioning of the histological samples and Prof. Michel Goedert for supplying the initial P301S mice to allow us to establish a colony.

REFERENCES

1. Brody, D. L., and Holtzman, D. M. (2008) *Annu. Rev. Neurosci.* **31,** 175–193
2. Thal, D. R., Holzer, M., Rüb, U., Waldmann, G., Günzel, S., Zedlick, D., and Schober, R. (2000) *Exp. Neurol.* **163,** 98–110
3. Hutton, M., Lendon, C. L., Rizzu, P., Baker, M., Froelich, S., Houlden, H., Pickering-Brown, S., Chakraverty, S., Isaacs, A., Grover, A., Hackett, J., Adamson, J., Lincoln, S., Dickson, D., Davies, P., Petersen, R. C., Stevens, M., de Graaff, E., Wauters, E., van Baren, J., Hillebrand, M., Joosse, M., Kwon, J. M., Nowotny, P., Che, L. K., Norton, J., Morris, J. C., Reed, L. A., Trojanowski, J., Basun, H., Lannfelt, L., Neystat, M., Fahn, S., Dark, F., Tannenberg, T., Dodd, P. R., Hayward, N., Kwok, J. B., Schofield, P. R., Andreadis, A., Snowden, J., Craufurd, D., Neary, D., Owen, F., Oostra, B. A., Hardy, J., Goate, A., van Swieten, J., Mann, D., Lynch, T., and Heutink, P. (1998) *Nature* **393,** 702–705
4. Goedert, M., Klug, A., and Crowther, R. (2006) *J. Alzheimers Dis.* **9,** 195–207
5. Asuni, A. A., Boutajangout, A., Quartermain, D., and Sigurdsson, E. M. (2007) *J. Neurosci.* **27,** 9115–9129
6. Boimel, M., Grigoriadis, N., Lourbopoulos, A., Haber, E., Abramsky, O., and Rosenmann, H. (2010) *Exp. Neurol.* **224,** 472–485
7. Boutajangout, A., Quartermain, D., and Sigurdsson, E. M. (2010) *J. Neurosci.* **30,** 16559–16566
8. Santacruz, K., Lewis, J., Spires, T., Paulson, J., Kotilinek, L., Ingelsson, M., Guimares, A., DeTure, M., Ramsden, M., McGowan, E., Forster, C., Yue, M., Orne, J., Janus, C., Mariash, A., Kuskowski, M., Hyman, B., Hutton, M., and Ashe, K. H. (2005) *Science* **309,** 476–481
9. Otvos, L., Jr., Feiner, L., Lang, E., Szendrei, G. I., Goedert, M., and Lee, V. M. (1994) *J. Neurosci. Res.* **39,** 669–673
10. Jicha, G. A., Weaver, C., Lane, E., Vianna, C., Kress, Y., Rockwood, J., and Davies, P. (1999) *J. Neurosci.* **19,** 7486–7494
11. Greenberg, S. G., and Davies, P. (1990) *Proc. Natl. Acad. Sci. U.S.A.* **87,** 5827–5831
12. Yamamori, H., Khatoon, S., Grundke-Iqbal, I., Blennow, K., Ewers, M., Hampel, H., and Iqbal, K. (2007) *Neurosci. Lett.* **418,** 186–189
13. Tremblay, M. A., Acker, C. M., and Davies, P. (2010) *J. Alzheimers Dis.* **19,** 721–733
14. Lewis, J., McGowan, E., Rockwood, J., Melrose, H., Nacharaju, P., Van Slegtenhorst, M., Gwinn-Hardy, K., Murphy, M. P., Baker, M., Yu, X., Duff, K., Hardy, J., Corral, A., Lin, W. L., Yen, S. H., Dickson, D. W., Davies, P., and Hutton, M. (2000) *Nat. Genet.* **25,** 402–405
15. Sahara, N., Lewis, J., DeTure, M., McGowan, E., Dickson, D. W., Hutton, M., and Yen, S. H. (2002) *J. Neurochem.* **83,** 1498–1508
16. Berger, Z., Roder, H., Hanna, A., Carlson, A., Rangachari, V., Yue, M., Wszolek, Z., Ashe, K., Knight, J., Dickson, D., Andorfer, C., Rosenberry, T. L., Lewis, J., Hutton, M., and Janus, C. (2007) *J. Neurosci.* **27,** 3650–3662
17. Goedert, M., Jakes, R., and Vanmechelen, E. (1995) *Neurosci. Lett.* **189,** 167–179
18. Le Corre, S., Klafki, H. W., Plesnila, N., Hübinger, G., Obermeier, A., Sahagún, H., Monse, B., Seneci, P., Lewis, J., Eriksen, J., Zehr, C., Yue, M., McGowan, E., Dickson, D. W., Hutton, M., and Roder, H. M. (2006) *Proc. Natl. Acad. Sci. U.S.A.* **103,** 9673–9678
19. Allen, B., Ingram, E., Takao, M., Smith, M. J., Jakes, R., Virdee, K., Yoshida, H., Holzer, M., Craxton, M., Emson, P. C., Atzori, C., Migheli, A., Crowther, R. A., Ghetti, B., Spillantini, M. G., and Goedert, M. (2002) *J. Neurosci.* **22,** 9340–9351
20. Reynolds, M. R., Reyes, J. F., Fu, Y., Bigio, E. H., Guillozet-Bongaarts, A. L., Berry, R. W., and Binder, L. I. (2006) *J. Neuosci.* **26,** 10636–10645
21. Rosenmann, H., Grigoriadis, N., Karussis, D., Boimel, M., Touloumi, O., Ovadia, H., and Abramsky, O. (2006) *Arch. Neurol.* **63,** 1459–1467
22. Bard, F., Cannon, C., Barbour, R., Burke, R. L., Games, D., Grajeda, H., Guido, T., Hu, K., Huang, J., Johnson-Wood, K., Khan, K., Kholodenko, D., Lee, M., Lieberburg, I., Motter, R., Nguyen, M., Soriano, F., Vasquez, N., Weiss, K., Welch, B., Seubert, P., Schenk, D., and Yednock, T. (2000) *Nat. Med.* **6,** 916–919
23. Wilcock, D. M., DiCarlo, G., Henderson, D., Jackson, J., Clarke, K., Ugen, K. E., Gordon, M. N., and Morgan, D. (2003) *J. Neurosci.* **23,** 3745–3751
24. Thompson, E. J., and Keir, G. (1990) *Ann. Clin. Biochem.* **27,** 425–435
25. Frost, B., Jacks, R. L., and Diamond, M. I. (2009) *J. Biol. Chem.* **284,** 12845–12852
26. Clavaguera, F., Bolmont, T., Crowther, R. A., Abramowski, D., Frank, S., Probst, A., Fraser, G., Stalder, A. K., Beibel, M., Staufenbiel, M., Jucker, M., Goedert, M., and Tolnay, M. (2009) *Nat. Cell Biol.* **11,** 909–913